Analysis on the dynamic mechanism of *Acetes* aggregation near a nuclear power cooling water system based on the Lagrangian flow network

Qi Lou[1,2], Xueqing Zhang[1,2]*, Xusheng Xiang[1,2], Fan Yu[1,3], Ying Xiong[4] and Zhengyan Li[1,2]

[1]College of Environmental Science and Engineering, Ocean University of China, Qingdao, China, [2]Key Laboratory of Marine Environment and Ecology, Ministry of Education of China, Ocean University of China, Qingdao, China, [3]State Key Laboratory of Nuclear Power Safety Monitoring Technology and Equipment, Shenzhen, China, [4]Marine and Fisheries Research Institute in Jiangsu Province, Nantong, China

The outbreak of nuclear power cooling water system (NPCS) disaster-causing organisms has become more frequent, causing huge economic losses. Therefore, it is necessary to understand the aggregation mechanism of disaster-causing organisms for the risk prevention and control of NPCS. Hence, this study applied the Lagrangian flow network (LFN) to analyze the aggregation mechanism of *Acetes* near NPCS, as such a complex network can describe the interconnections between massive nodes and has already been used for modeling complex nonlinear systems, revealing how the mechanisms of such novel processes emerge. In this study, the degree and probability paths in the network were used to reveal the transport pathway and aggregation area of *Acetes*. The experimental results highlighted that the sea area of the nuclear power plant is the key node with a large in-degree of the LFN, where the material easily accumulated. The *Acetes* near the NPCS mainly originated from the east along two critical paths. Overall, this study demonstrates that the LFN is a feasible approach to predicting the transport and the accumulation of the NPCS disaster-causing plankton.

KEYWORDS

complex flow network, Lagrangian particle tracking, *Acetes chinensis*, nuclear power plant cooling system

1 Introduction

According to the 2022 world nuclear industry status report, in 2021, the world's nuclear power plants generated 2,653 billion kilowatt-hours of electricity, constituting 9.8% of the total electricity generated (Schneider et al., 2016). Most nuclear power plants are located in coastal areas to utilize seawater as the cooling water source, imposing challenges to the safe

operation of seawater intake. In recent years, marine biological outbreaks have blocked the cold source seawater intake of nuclear power plants, affecting the safe and stable operation of such power plants from time to time (Azila and Chong, 2010; Barath Kumar et al., 2017). Blockage of the cold source seawater intake of coastal nuclear power plants mainly involves algae, jellyfish, *Acetes*, seagrass, sand, ice, and crude oil, among others, of which these marine organisms are the main causes, accounting for 84% of the blocking events (An et al., 2021). In China, the nuclear power plants at Hongyanhe, Ningde, Fangchenggang, and Yangjiang have been shut down several times due to the blockage of the cooling water intakes caused by blooms of jellyfish, sea cucumbers, algae, and *Acetes*, respectively (Zeng et al., 2019; An et al., 2021; Wang et al., 2021). Specifically, due to their high biological density, short growth period, fast growth rate, and small size, *Acetes* are the most challenging disaster-causing organisms that should be controlled. Thus, this study focused on the *Acetes* near a nuclear power cooling water system (NPCS) and analyzed their transport, aggregation, and outbreak mechanisms.

Studies on the transport and mechanism of *Acetes* have received more attention in recent years. One of the research approaches is ocean investigation, such as the trawl method, underwater visual census techniques (Edgar et al., 2004; Tessier et al., 2013), acoustic method (Zeng et al., 2019), and the vessel monitoring system (VMS) (Fonseca et al., 2008; Li et al., 2022). An alternative research approach is employing a statistical model in which a species distribution model (SDM), such as BIOCLIM (bioclimatic modeling), DOMAIN (domain environmental envelope), GARP (genetic algorithm for rule-set production), CLIMEX (climate change experiment), and MaxEnt (maximum entropy) (He et al., 2021), utilizes the known species distribution data and relevant environmental variables to determine the spatial niche of species. However, this statistical model cannot reveal the dynamic mechanisms. Therefore, the particle tracking model (Hufnagl et al., 2017) or the individual-based model (IBM) (El Saadi and Bah, 2006; Falcini et al., 2020) is often applied to study the transport of biological particles, but describing the transport pathway and the connectivity between regions from complex particle trajectories is quite difficult.

This work utilized the Lagrangian flow network (LFN) theory to study the transport of *Acetes*. The LFN describes the fluid flow or material exchange among different locations, which is defined as a flow network or transport network. In the LFN, small regions in the fluid domain are interpreted as vertices, and the mass transfer from one of these regions to another defines the weighted links among them (Ser-Giacomi et al., 2015a). Based on the network, the material transport convert to the characteristics of the complex networks. Hence, a lot of powerful tools from the graph theory are available for analysis of the material transport processes. Over the past decade, the LFN theory has been successfully applied to analyze turbulent mixing (Iacobello et al., 2019), ocean transport in the Mediterranean (Ser-Giacomi et al., 2015b), and ocean surface connectivity in the Arctic (Reijnders et al., 2021), etc.

In this study, the prognostic, unstructured grid, finite-volume, free-surface, three-dimensional primitive equation coastal ocean circulation model (FVCOM) was used to obtain the current field of the study area, and the LFN approach was applied to detect the structures of the material transport, including the degrees, betweenness, and connectivity.

This paper is organized as follows. *Section 1* introduces the background of the NPCS disaster-causing organisms. *Section 2* introduces the hydrodynamic model and the LFN approach. *Section 3* shows the results of the distribution, the pathway, and the source of the *Acetes* particles. *Section 4* includes the discussion and conclusion.

2 Materials and methods

The LFN framework requires the calculation of the material transport process in the whole domain and then uses a number of mathematical methods to map the material transport process into the edges of the network. The first step in calculating the material transport process is to obtain the hydrodynamic field with a high spatial and temporal resolution, which can only be derived from the ocean circulation model. Therefore, the FVCOM was introduced in this study.

2.1 Hydrodynamic model

FVCOM was applied to obtain the hydrodynamic field in this study. The hydrodynamic equations were numerically resolved on unstructured grids using the finite-volume method. Because of the advantage of the body-fitted grid, FVCOM is widely used in estuarine and coastal areas. In addition, the finite-volume algorithm guarantees volume and mass conservation of the momentum fluxes. The reader is referred to Chen et al. (2003) for further details on the governing equations.

In this study, the model area is located 111.86°–112.97° E, 21.45°–22.02° N (Figure 1), which comprised 4,505 nodes and 8,172 triangles (elements) with 200 m minimum horizontal grid resolution and five uniform σ layers. Horizontal diffusion was parameterized based on Smagorinsky's formation, and vertical turbulent mixing was calculated with the 2.5-level Mellor and Yamada turbulence model. The tide level data on the boundary were taken from the TMD toolbox (Tidal Model Driver) (Padman, 2005) with the TPXO7 global tide model, which included eight tidal constituents (M_2, S_2, K_1, O_1, P_1, Q_1, N_2, and K_2). The sea surface wind data were extracted from the ERA5 (European Centre for Medium-Range Weather Forecasts) reanalysis dataset. The drainage water of the NPCS was also included in the model, with the flux set as 350 m³/s (Chen et al., 2013) at a temperature of 8°C higher than natural environment seawater.

FVCOM produced a three-dimensional hydrodynamic field hourly. Subsequently, the surface current field was extracted and interpolated to drive a particle tracking model to simulate the drifting process of *Acetes*, which was then used in the construction of the LFN.

2.2 Construction of the Lagrangian flow network

The network, also called the graph in mathematics, is a set of points joined together in pairs by lines. The points are referred to as vertices or nodes and the lines referred to as edges or links. Many objects of interest in the physical, biological, and social sciences can be considered as networks (Newman, 2010). The adjacency matrix is the
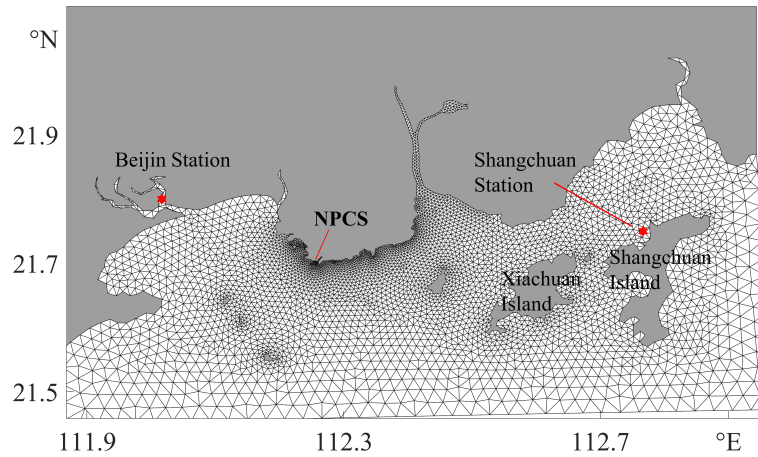
FIGURE 1
Model grid in the study area.

most common representation of a network. The adjacency matrix A is the matrix with elements A_{ij}:

$$A_{ij} = \begin{cases} 1, \text{if there is an edge between vertices } i \text{ and } j \\ 0, \quad \text{otherwise} \end{cases} \quad (1)$$

The network constructed by A_{ij} is unweighted. Similarly, the weight matrix representing the strength of the connection between vertices i and j is denoted as W_{ij}:

$$W_{ij} = \begin{cases} 1, \text{if the weitht of the link}(i,j) \text{ is } W_{ij} \\ \quad\quad 0, \text{ otherwise} \end{cases} \quad (2)$$

In the ocean, one way to establish the network is to base it on the particle transport dynamics, in which the nodes correspond to discretized domains and the links are defined by the connectivity between the regions (Ser-Giacomi et al., 2015a). The research domain was divided into 831 sub-regions (Figure 2) with an area of 4 km^2. A total of 250,000 particles were seeded in the domain, and all particles were tracked from time t_0 March 1) to time t (March 30). The

swimming speed of *Acetes* was far less than the flow velocity, so that they are considered as being passively advected by the sea current:

$$\frac{d\vec{x}}{dt} = \vec{v}(\vec{x}(t), t) \quad (3)$$

where $\vec{x}$ is the displacement vector of the particles at time t and $\frac{d\vec{x}}{dt}$ the derivative of the displacement vector $\vec{x}$ to time t. The $\vec{v}$ is the velocity of the particle coming from the FVCOM output.

For any particle that moves from V_i to V_j, the connection from V_i to V_j is established defining the edge E_{ij} ($A_{ij} = 1$). However, it should be emphasized that the link in the network is directed, which means that the link from V_i to V_j is not the same as that from V_j to V_i. Moreover, the weight of the links is defined by the transport probability of particles from vertex V_i to V_j:

$$W_{ij}(t_0, \tau) = P_{ij}(t_0, \tau) = \frac{N_{ij}}{N_i} \quad (4)$$

where N_{ij} is the number of particles from V_i to V_j and N_i is the initial number of particles in V_i. $P_{ij}(t_0,\tau)$ is regarded as the weight of the link from node V_i to node V_j. Subsequently, the network described by a transport matrix $P(t_0,\tau)$ as constructed.
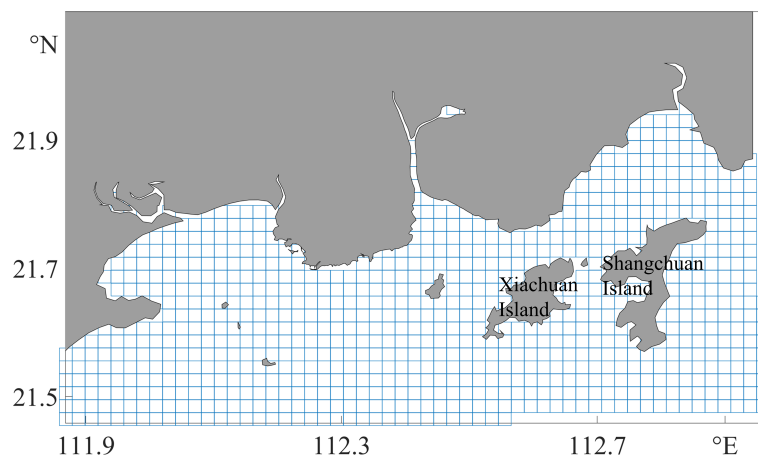

FIGURE 2
Vertices of the Lagrangian flow network (LFN) in the study area.

3 Results

3.1 Model validation

3.1.1 Water level validation

Tide is the most prominent driving factor of the current field offshore. Therefore, we verified the model based on the tidal level. The tide observation data, covering the period from December 20 to December 30, 2019, were obtained from the National Marine Data Center. Figure 1 illustrates the tide stations, while Figure 3 compares the simulation and the observation results, highlighting that the results of the model fitted well with the observations. The mean Pearson's correlation coefficient for the two-site data was 0.9616, and the root mean square error (RMSE) values were 0.18 and 0.10 m for the Beijin and Shangchuan stations, respectively.

3.1.2 Tidal current validation

The M_2 and K_1 tide components dominated the current in the investigated research domain. We calculated the tide current ellipse of these tide components based on the output of the FVCOM, and the observation data were derived from an environmental impact assessment report conducted near the nuclear power plant (Zhang, 2021). The *in situ* investigation started on June 21 and ended on June 23, 2020. The parameters including the major axis length, the minor axis length, and the orientation of the tidal ellipses based on the observation data were provided in this report. The tidal ellipses at three observation stations were calculated from the model output as well for comparison.

As seen in Figure 4, the M_2 tidal current component with a speed of about 20 cm/s contributed the majority of the tidal current, and the average speed of the K_1 tide ellipses was about 10 cm/s. The tide ellipse orientations of the model and the observation were similar, which were both parallel to the coastline, and the difference of the ellipse axis length between the simulated and measured values was not obvious, confirming the validity of the FVCOM from the other side. Quantitatively, for M_2 and K_1, the RMSE values of the tide ellipse major axis length were 3.09 and 2.40 cm/s, respectively, while those of the tide ellipse orientation were 15.26° and 3.72°, respectively. In

conclusion, the hydrodynamic model can provide reliable hydrodynamic fields for subsequent analysis.

3.2 Tidal current field

Figure 5 depicts the flow field distribution at ebb time and flood time during the spring tide in the simulated area. At flood time, the current flowed from the southeast to northwest, and at ebb time, the flow direction is in reverse. During flood time, the flow velocity in the whole field was mostly at 0–0.4 m/s, which can reach 0.4–0.8 m/s in the area around the NPCS and Xiachuan Island due to the influence of topography. The velocity during the ebb time was lower than that during flood time.

3.3 Transport of virtual *Acetes* particles

To clearly describe the transport and distribution of *Acetes* near the nuclear power plant, this study utilized a Lagrangian particle tracking model using passive particles to represent the *Acetes*. The particles were seeded in a uniform distance of 200 m and ran for 30 days, with March 1, 2020, as the initial release moment. Figure 6 shows the distribution of the particles for 3, 7, 15, and 30 days after releasing the particles.

The particles were mainly transported offshore for 3 days in the study area. After 7 days, the particles started showing a spatial dispersion near the coast, with some striped distribution structures. Figures 6C, D indicate obvious strips of structures where the aggregation of the particles occurred near the sea entry of three rivers. In contrast, the particles at the estuary spread rapidly, and the number of remaining particles was very small. The particles were mostly in patched aggregates near several islands on the eastern side of the study area. Since *Acetes* are poor swimmers and can be considered as plankton whose transport and distribution are controlled by currents, the particle tracking results can represent their trajectories in this region.

3.4 Out-degree and in-degree

The degree of a vertex in a graph is the number of edges connected to it. In a directed network, the connectivity of each vertex is described by both the in-degree and the out-degree. The in-degree k_i^{in} of vertex i is the number of edges arriving at i while the out-degree k_i^{out} of vertex i is the number of outgoing edges from i. In terms of the adjacency matrix A_{ji} the in-degree and out-degree can be written as:

$$k_i^{\text{in}} = \sum_{j=1}^{n} A_{ji} \tag{5}$$

$$k_i^{\text{out}} = \sum_{j=1}^{n} A_{ij} \tag{6}$$

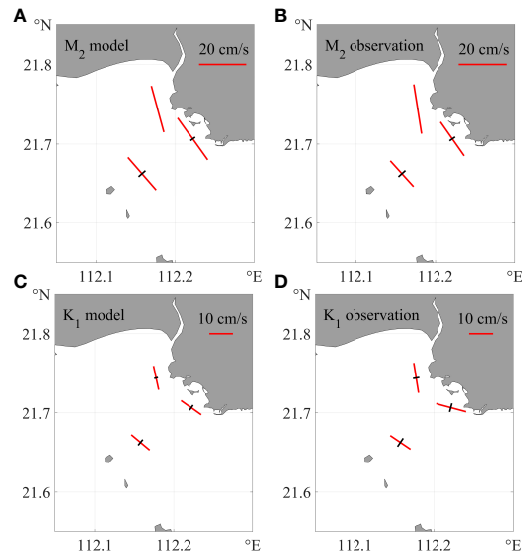The degree of a vertex has an immediate interpretation considering centrality, quantifying how well an element is

FIGURE 3
Tidal level validation at Beijin station **(A)** and Shangchuan Island station **(B)**.
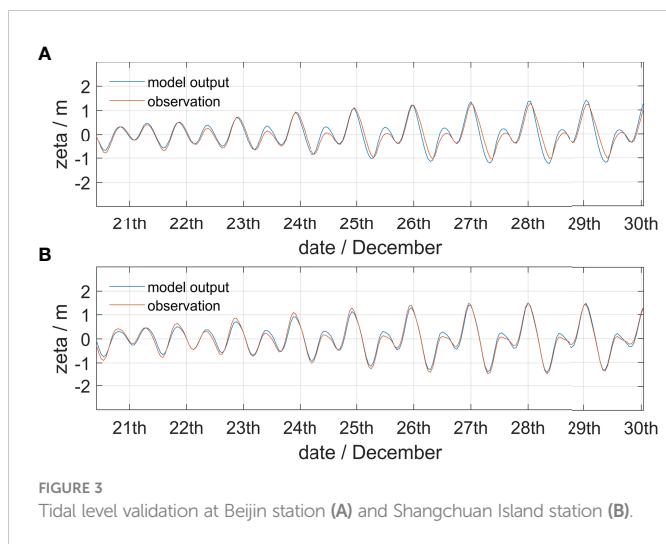
FIGURE 4
Tidal current ellipses obtained through both model simulation and observation. **(A)** Model output of the M₂ tide ellipse. **(B)** Observation of the M₂ tide ellipse. **(C)** Model output of the K₁ tide ellipse. **(D)** Observation of K₁.

connected to the other elements in the graph (Barrat et al.). Regarding the LFN that corresponds to the aggregation and diffusion of materials in the ocean, the vertex with a large in-degree implies that the material easily accumulates there, which is generally considered as a "sink" in the description of ocean material transport; in contrast, a large out-degree indicates that the vertex can be considered as a "source".

Figure 7 illustrates the distribution of the in-degree and out-degree within 30 days. The degrees were mostly less than 10, and

vertices with a large degree are likely to be near the coast. Figure 7 also highlights that the in-degree and out-degree were higher at offshore areas, i.e., sea areas where the cooling system is located that act both as a "sink" and as a "source" of the materials around them. From a network's perspective, it is the hub vertex in the material transport process. If any environmental variations influence the nearby material transport, for instance, reducing the diffusion process, the materials will be continuously convected inwards because of the large in-degree, but not outwards due to the limited diffusion process. The NPCS is in an unstable equilibrium condition, and this material transport pattern brings with it a high risk of natural outbreak of these organisms.
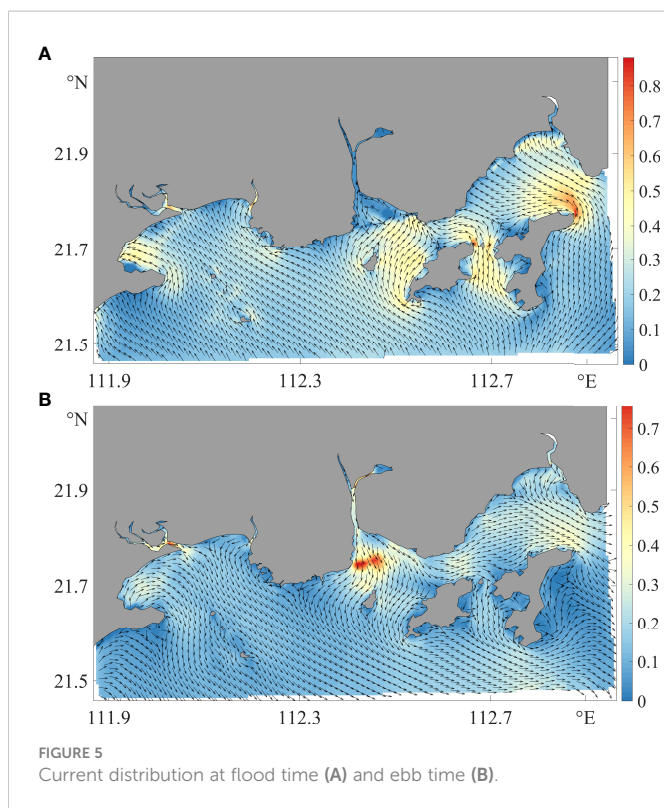
3.5 The path and source of *Acetes*

A path in a network is any sequence of vertices so that every consecutive pair of vertices in the sequence is connected by an edge in the network (Newman, 2010). The path is often used to analyze the connectivity among vertices, and the path concept depends on the distances among vertices. In the ocean, the distance is not limited to the Euclidean distance, as the shortest time to the fastest path or the most probable path (MPP) is more meaningful in practice. This study applied the MPP to determine the optimum path.

When all paths connected to the location of the nuclear power plant were found, we collected their starting points and labeled them as the source of *Acetes* (red dots in Figure 8). Obviously, the results depend on the integration time. Considering the results within 30 and 90 days, the potential source area was located east of the nuclear power plant, which covered an area of about 120 km², and within 90 days, the area was about 475 km².

In order to determine the path, we introduced another network metric, the betweenness centrality. Betweenness measures the extent to which a vertex lies on the key paths between other vertices. Mathematically, if N_{jl} s the total number of the MPPs (Ser-Giacomi et al., 2015b) from V_j o V_l and $N_{jl}(i)$ is the number of these MPPs that
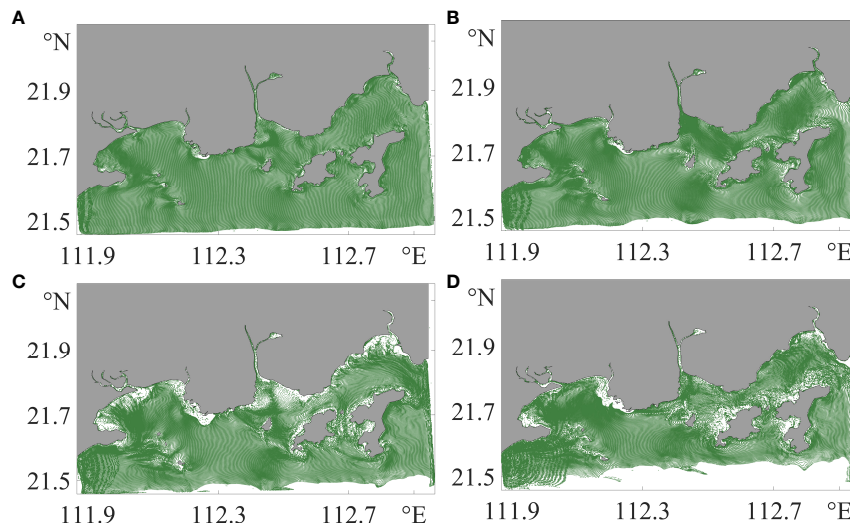

FIGURE 5
Current distribution at flood time **(A)** and ebb time **(B)**.

FIGURE 6
Distribution of the virtual *Acetes* particles for integration times of 3 days **(A)**, 7 days **(B)**, 15 days **(C)**, and 30 days **(D)** since March 1, 2020.

pass through the V_i the betweenness of V_i is defined as:

$$B_i = \sum_{\substack{\forall j, l \\ j \neq l \neq i}} \left[N_{jl}(i)/N_{jl} \right] \qquad (7)$$

Vertices with high betweenness pose a greater influence within a network. On the other hand, in terms of the ocean, betweenness is a measure of the hidden bottlenecks of the material transport system, and aligned high-betweenness vertices indicate the major material

FIGURE 7
Distribution of in-degree **(A)** and out-degree **(B)**.

transport pathways (Ser-Giacomi et al., 2021). Hence, the betweenness is critical in the analysis of material transport and in the determination of the ocean's flow structure.

As mentioned above, the *Acetes* near the nuclear power plant originated from the east with a large probability. The betweenness results showed that the organisms were not uniformly or randomly transported to the nuclear power plant's sea area. Instead, two clear transport pathways (Figure 9) passed through the sea area of the nuclear plant. The first pathway goes along the coast that extends to the eastern boundary of the research domain, while the other bypasses the southern edges of Xiachuan Island and merges with the first pathway just near the NPCS. The two pathways formed a "-<"-shaped transport structure, and the intersection of two major material transport pathways was only about 10 km from the NPCS. Most of the time, this "-<"-shaped pathway carries materials westward and works in balance. However, when any environmental interruptions such as coast-pointing winds occur, this fragile system falls into unbalance and the material flow is cut off, which might result in an organism aggregation or even in a harmful outbreak. The effect of wind direction will be discussed in the next section.

3.6 Discussion

The distribution of *Acetes* is affected by biological, chemical, and physical factors, with their outbreak mechanism still being poorly understood. In this study, we focused on the dynamic factors. Figure 10 reveals the relationship between wind and the daily catch of *Acetes* from 2020 to 2021. The *Acetes* catch data were provided by the State Key Laboratory of Nuclear Power Safety Monitoring Technology and Equipment, and the wind data around the NPCS were extracted from the ERA5 reanalysis data. An *Acetes* outbreak is most likely to happen in late winter or in early spring, so we aimed to analyze and determine what happens during these periods. We hypothesized that the temperature and the material transport
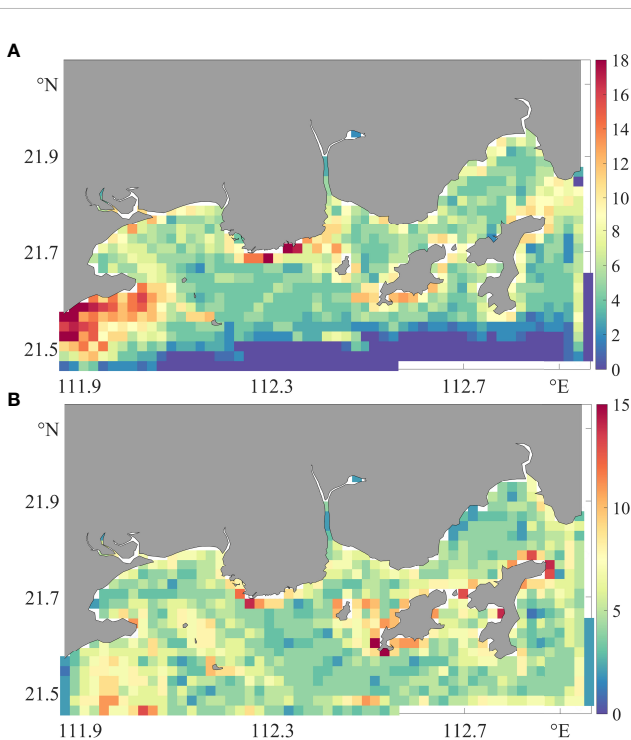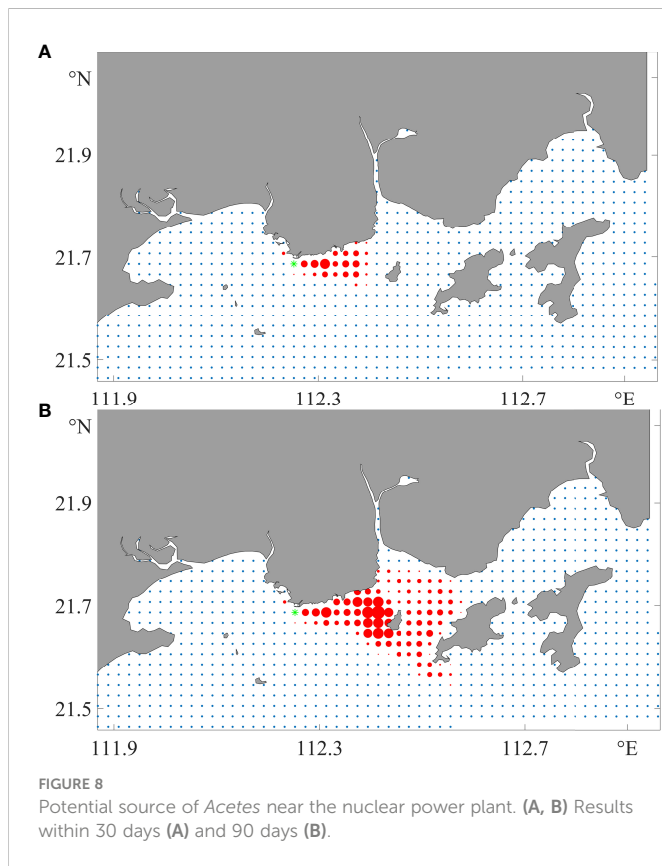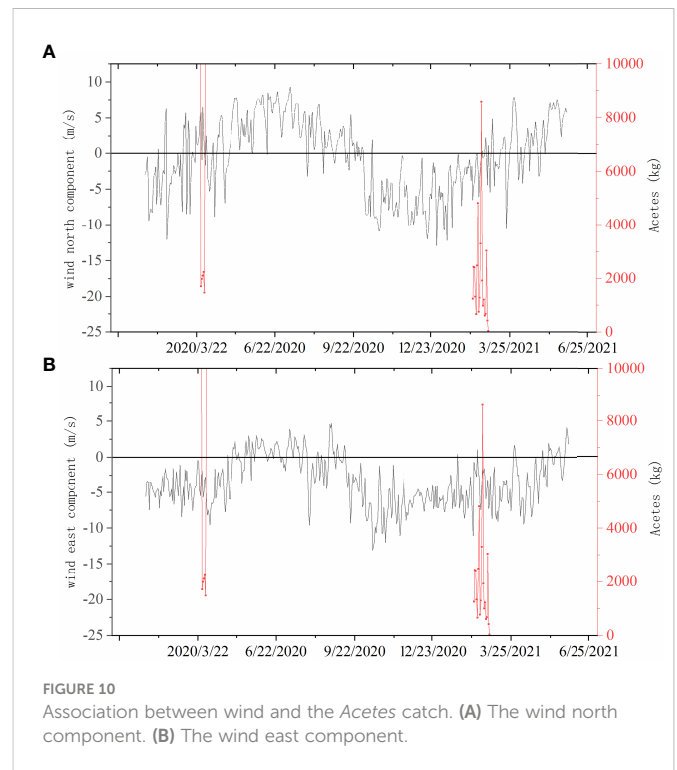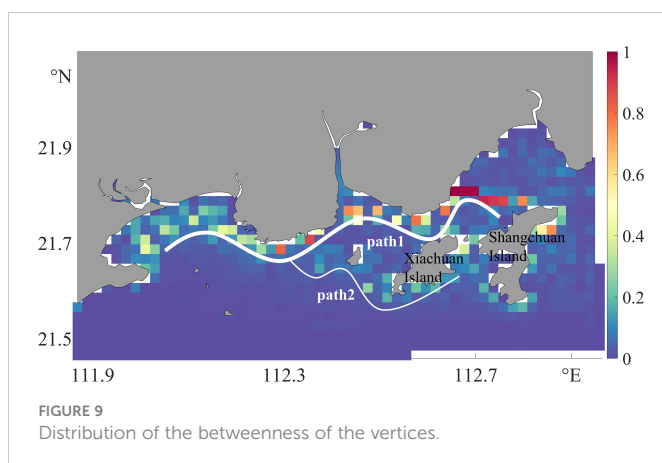
FIGURE 8
Potential source of *Acetes* near the nuclear power plant. **(A, B)** Results within 30 days **(A)** and 90 days **(B)**.

FIGURE 10
Association between wind and the *Acetes* catch. **(A)** The wind north component. **(B)** The wind east component.

pattern are the intrinsic causes, and wind is an acceleration factor. Intriguingly, the outbreak of *Acetes* showed a strong relationship with the time when the winds are turning from northeast to southwest. Wind stress turning from offshore to onshore influenced the material transport pattern; that is, the two major pathways intersected in the cooling system, thus causing the aggregation of *Acetes* around it. Afterward, with the reversed wind direction, the old transport pattern was destructed and the seawater temperature also rose too high for *Acetes* to survive, explaining the reduction in the daily catch of *Acetes*.

Subsequently, we ran a parallel experiment that removed the surface wind on the ocean to clarify the model's sensitivity to wind. The configurations of the hydrodynamic model and the network were the same, except for the removal of the surface wind stress. The two

experiments were denoted as the "with-wind" case and the "no-wind" case.

On the one hand, Figure 11 depicts the betweenness pathways in the no-wind experiment, where the shape of the pathways was similar to that in the with-wind experiment, which is a two-pathway flow from the east to the west conjunct in the middle; however, the pathways in the no-wind experiment were shifted two or three grids to the south and thus staggered the NPCS. Most materials transported westward will not go through the NPCS, if the wind is weak. Therefore, the *Acetes* had a small probability of touching the NPCS or even break out without the assistance of the northwestward winds.

On the other hand, the in-degree and out-degree of the network, which depict the characteristic of the aggregation and diffusion processes of *Acetes*, also made significant changes under the influence of wind. When wind was added to the model, the in-degree, which represents the sink of a material, increased significantly (Figures 12A, B). However, the out-degree, which represents the source of the material, decreased by about 50% when wind was included (Figures 12C, D). To sum up, the extra northwestward wind increased the extent of the material sink and decreased the extent of the material source near the NPCS.

4 Conclusion

This paper applied the LFN theory to study the transport and aggregation mechanism of *Acetes* near a nuclear power plant. The LFN is a feasible and novel method used to predict the spatial and temporal distribution of plankton, such as the pelagic larva and *Acetes*. Particularly, LFN can detect the material transport path and
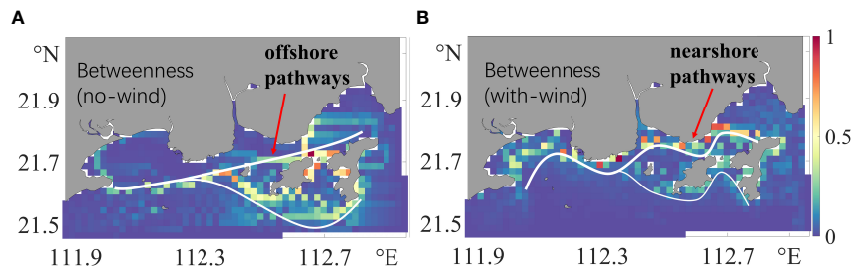

FIGURE 9
Distribution of the betweenness of the vertices.

FIGURE 11
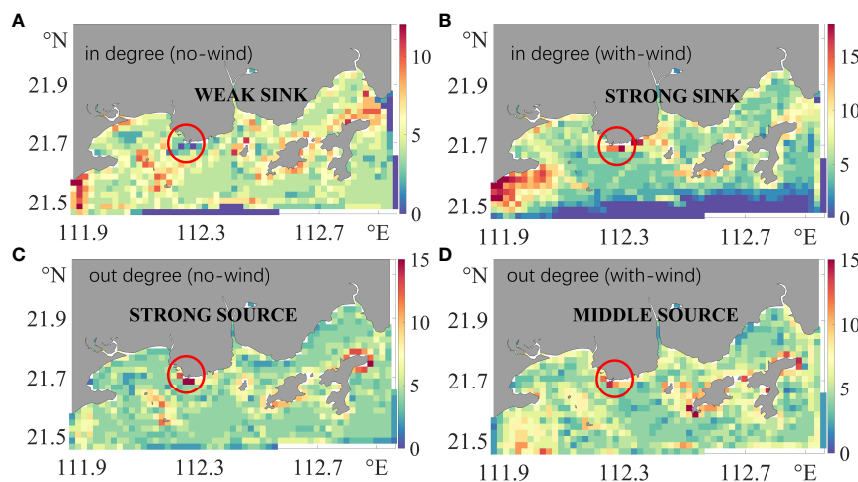The betweenness pathways with wind in March **(B)** and without wind **(A)**.

FIGURE 12
In-degree **(A, B)** and out-degree **(C, D)** under the no-wind and with-wind experiments.

trace the origin of disaster-causing organisms, which cannot be achieved using circulation or particle tracking methods.

The degree of LFN illustrates the importance of the vertex in the network, which corresponds to the aggregation or the diffusion characteristic. In this study, the cooling water intake of the nuclear power plant comprised just the high in-degree and high out-degree nodes, representing a large material diffusion ability and accumulation probabilities. Hence, any small perturbation destroys the nearby mass balance, and thus a large amount of material might be immediately accumulated near the area.

From the perspective of betweenness, the cooling water intake of the nuclear power plant was located at the junction of the two pathways. The materials were transported from the east to the west and from the south to the north, forming a "-<"-shaped transport structure (see Figure 9) and passing through the sea area of the nuclear power plant. When the external environment changes, e.g., the wind direction suddenly changes from the offshore wind to the onshore wind, the materials transported from the pathway will accumulate near the coast under the effect of wind. This phenomenon has also been confirmed by observation.

Nevertheless, we suppose that the wind direction might be an important factor causing the outbreak of *Acetes*; that is, at a suitable

temperature, the southeast wind will cause the aggregation of *Acetes* in the study area.

Data availability statement

The raw data supporting the conclusions of this article will be made available by the corresponding author, without undue reservation.

Author contributions

XZ proposed the idea of using the Lagrangian flow network on the *Acetes* near the nuclear power cooling water system and wrote the manuscript. QL ran the hydrodynamic model and wrote the context in this paper. XX established the LFN model and plotted the figures in this paper. FY recorded and provided precious long-term observation data on *Acetes*. ZL proposed some valuable suggestions in revising this article. YX provided some important information about the habits of *Acetes* and helped revise the introduction part. All authors contributed to the article and approved the submitted version.

Funding

Acknowledgments

Conflict of interest

The authors declare that the research was conducted in the absence of any commercial or financial relationships that could be construed as a potential conflict of interest.

Publisher's note

All claims expressed in this article are solely those of the authors and do not necessarily represent those of their affiliated organizations, or those of the publisher, the editors and the reviewers. Any product that may be evaluated in this article, or claim that may be made by its manufacturer, is not guaranteed or endorsed by the publisher.

References

An, L., Wang, L., Ou, D., Jia, C., Li, W., Ding, Y., et al. (2021). The ecological mechanisms of acetes blooms as a threat to the security of cooling systems in coastal nuclear power plants. *J. Coast. Conserv.* 25, 55. doi: 10.1007/s11852-021-00845-0

Azila, A., and Chong, V. C. (2010). Multispecies impingement in a tropical power plant, straits of malacca. *Mar. Environ. Res.* 70, 13–25. doi: 10.1016/j.marenvres.2010.02.004

Barath Kumar, S., Mohanty, A. K., Das, N. P. I., Satpathy, K. K., and Sarkar, S. K. (2017). Impingement of marine organisms in a tropical atomic power plant cooling water system. *Mar. pollut. Bull.* 124, 555–562. doi: 10.1016/j.marpolbul.2017.07.067

Barrat, A., Lemy, M. B., and Vespignani, A. (2008). DYNAMICAL PROCESSES ON COMPLEX NETWORKS Cambridge university press. 367.

Chen, C., Liu, H., and Beardsley, R. C. (2003). An unstructured grid, finite-volume, three-dimensional, primitive equations ocean model: Application to coastal ocean and estuaries. *J. Atmospheric Ocean. Technol.* 20, 159–186. doi: 10.1175/1520-0426(2003) 020<0159:AUGFVT>2.0.CO;2

Chen, X., Tang, S., and Ou, D. (2013). Assessment report of yangjiang nuclear power plant project on fishery resources and ecology in adjacent waters.

Edgar, G. J., Barrett, N. S., and Morton, A. J. (2004). Biases associated with the use of underwater visual census techniques to quantify the density and size-structure of fish populations. *J. Exp. Mar. Biol. Ecol.* 308, 269–290. doi: 10.1016/j.jembe.2004.03.004

El Saadi, N., and Bah, A. (2006). On phytoplankton aggregation: A view from an IBM approach. *C. R. Biol.* 329, 669–678. doi: 10.1016/j.crvi.2006.05.004

Falcini, F., Corrado, R., Torri, M., Mangano, M. C., Zarrad, R., Di Cintio, A., et al. (2020). Seascape connectivity of European anchovy in the central Mediterranean Sea revealed by weighted Lagrangian backtracking and bio-energetic modelling. *Sci. Rep.* 10, 18630. doi: 10.1038/s41598-020-75680-8

Fonseca, T., Campos, A., Afonso-Dias, M., Fonseca, P., and Pereira, J. (2008). Trawling for cephalopods off the Portuguese coast–fleet dynamics and landings composition. *Fish. Res.* 92, 180–188. doi: 10.1016/j.fishres.2008.01.015

He, Y., Liu, S., Yuan, Y., Jiang, K., Wang, T., Qin, Y., et al. (2021). The potential suitability habitat prediction of acaudina molpadioides based on maxent model. *Haiyang Xuebao* 43, 65–74.

Hufnagl, M., Payne, M., Lacroix, G., Bolle, L. J., Daewel, U., Dickey-Collas, M., et al. (2017). Variation that can be expected when using particle tracking models in connectivity studies. *J. Sea Res.* 127, 133–149. doi: 10.1016/j.seares.2017.04.009

Iacobello, G., Scarsoglio, S., Kuerten, J. G. M., and Ridolfi, L. (2019). Lagrangian Network analysis of turbulent mixing. *J. Fluid Mech.* 865, 546–562. doi: 10.1017/ jfm.2019.79

Li, G., Li, D., Xiong, Y., Zhong, X., Tang, J., Song, D., et al. (2022). Changes in the resource distribution of acetes chinensis and patterns of species replacement in haizhou bay in summer based on BeiDou VMS data. *Reg. Stud. Mar. Sci.* 56, 102655. doi: 10.1016/ j.rsma.2022.102655

Newman, M. E. J. (2010). *Networks: An introduction* (Oxford, New York: Oxford University Press).

Padman, L. (2005) *Tide model driver (TMD) manual*. Available at: https://svn.oss. deltares.nl/repos/openearthtools/trunk/matlab/applications/DelftDashBoard/utils/tmd/ Documentation/README_TMD_vs1.2.pdf.

Reijnders, D., van Leeuwen, E. J., and van Sebille, E. (2021). Ocean surface connectivity in the Arctic: Capabilities and caveats of community detection in Lagrangian flow networks. *J. Geophys. Res. Oceans* 126. doi: 10.1029/2020JC016416

Schneider, M., Froggatt, A., Hosokawa, K., Thomas, S., Yamaguchi, Y., and Hazemann, J. (2016). The world nuclear industry status report. *Mycle Schneider Consult. MSC* 12, 124–128.

Ser-Giacomi, E., Baudena, A., Rossi, V., Follows, M., Clayton, S., Vasile, R., et al. (2021). Lagrangian Betweenness as a measure of bottlenecks in dynamical systems with oceanographic examples. *Nat. Commun.* 12, 1–14. doi: 10.1038/s41467-021-25155-9

Ser-Giacomi, E., Rossi, V., López, C., and Hernández-García, E. (2015a). Flow networks: A characterization of geophysical fluid transport. *Chaos Interdiscip. J. Nonlinear Sci.* 25, 036404. doi: 10.1063/1.4908231

Ser-Giacomi, E., Vasile, R., Hernández-García, E., and López, C. (2015b). Most probable paths in temporal weighted networks: An application to ocean transport. *Phys. Rev. E Stat. Nonlin. Soft Matter Phys.* 92, 12818. doi: 10.1103/PhysRevE.92.012818

Tessier, A., Pastor, J., Francour, P., Saragoni, G., Crec'hriou, R., and Lenfant, P. (2013). Video transects as a complement to underwater visual census to study reserve effect on fish assemblages. *Aquat. Biol.* 18, 229–241. doi: 10.3354/ab00506

Wang, J., Ma, C., and Zou, Q. (2021). Status and suggestions of cold source safety guarantee for nuclear power plants in south China. *Nucl. Saf.* 20, 65–71. doi: 10.16432/ j.cnki.1672-5360.2021.03.012

Zeng, L., Chen, G., Wang, T., Yang, B., Yu, J., Liao, X., et al. (2019). Acoustic detection and analysis of acetes chinensis in the adjacent waters of the daya bay nuclear power plant. *J. Fish. Sci. China* 26, 1029–1039.

Zhang, (2021). *Environmental impact assessment report on the rescue and reinforcement project of baishatou revealment of dongping national central fishing port in yangjiang city (Phase III)* (Tianjin: Sea Island Environmental Science and Technology Research Institute (Tianjin).